# SLOPED GRANULAR OPEN FILTERS UNDER WAVE LOADING

Guido Wolters[1], Marcel R.A. van Gent[2], Jelle Olthof[3], Gregory M. Smith[4]

Rubble mound coastal structures typically contain granular filters in one or more layers. These filters are normally geometrically tight (to prevent material washout), often difficult to realize in the field, and expensive. An alternative is a geometrically open filter. A geometrically open filter has a large ratio of the size of toplayer material and underlayer material and is designed in such a way that it fulfills its filter functions with only minimal base material loss or settlement. Potential applications of open filters include bed protections and toe & slope configurations of coastal structures. Proper guidelines on the design of open filters under wave loading could lead to significant cost and material savings, and to a more practical application of filters in the field. Physical model tests were conducted in a wave flume. These tests focussed on granular open filters on a 1:7 sand slope under wave loading. The analysis of the tests has led to guidelines on the amount of erosion of the sand underneath a granular filter and of the sand accretion within a granular filter.

*Keywords: rubble-mound breakwater; revetment; open filter; transport filter; waves; physical model tests*

## INTRODUCTION

Rubble mound structures typically contain granular filters. These filters fulfil several functions. They prevent the erosion (washing out) of finer base material or sub-layers due to waves and currents, contribute to the energy dissipation by turbulent flow through the voids, and provide drainage. Granular filters can be designed as geometrically tight filters or geometrically open filters. Open filters are either hydraulically closed filters, in which the threshold value for incipient motion of base material is not exceeded, or transport filters, in which transport of base material occurs.

The design of geometrically tight filters (no material washout) is relatively straightforward, but in many instances a large number of filter layers and material volume is required. Each layer should have a minimum thickness of at least a few diameters but for practical reasons also a minimum thickness irrespective of the size of the material (*e.g.* 0.5 m) is required. For a granular filter of a number of layers, the latter minimum thickness may lead to a substantial size of the total filter. One alternative is a geometrically open filter in which no transport of sand occurs because the hydraulic load is smaller than the threshold value for incipient motion (hydraulically closed filter). Another alternative is a transport filter where some movement of sand within or even out of the granular filter layer is allowed. In this case the hydraulic load is larger than the threshold value for incipient motion. The design of a transport filter is based on the principle that the hydraulic loading is such that erosion of base material (or settlement) remains below an acceptable level. In practice, limited settlement is often permitted. Typical applications of transport filters include for instance toe and slope configurations of coastal structures as well as bed protections.

In the 1980s and 1990s a large number of tests have been performed by for instance De Graauw *et al.* (1983), Bakker *et al.* (1994) and Klein Breteler *et al.* (1992) to determine criteria for the initiation of motion in granular filters. These criteria are based on estimates of the hydraulic gradients parallel or perpendicular to the interface between sand and the granular filter. This has resulted in various formulae and a design diagram for interface stability of granular filters, see for instance CUR Report 161 (1993). Furthermore, new criteria for interface stability have been introduced in CUR Report 233 (2010) and Van de Sande (2012). These studies have been conducted with a focus on steady flow and the beginning of base material transport through the filter. The studies do, therefore, not specifically address material transport itself or effects of filter settling. However, several transport measurements have been conducted but these were mainly for small transported volumes and for non-cyclic loading. Very little knowledge is available about critical hydraulic gradients and material transport for cyclic (unsteady) processes.

An overview of the available design methods and knowledge gaps can be found in Wolters (2012). Proper guidelines on the design of open transport filters, that allow an acceptable and

[1] Deltares, Delft, The Netherlands, guido.wolters@deltares.nl
[2] Deltares, Delft, The Netherlands, marcel.vangent@deltares.nl
[3] Boskalis Westminster, The Netherlands, j.olthof@boskalis.nl
[4] Van Oord, The Netherlands, greg.smith@vanoord.com

predictable loss of base material under wave and current loading, could lead to significant cost and material savings, and to a more practical application of filters in the field. As a step towards guidelines for open filters under wave loading a joint project (JIP-Topfilter) has been executed. Partners of this project are Deltares, Boskalis, Van Oord, Witteveen+Bos, Rijkswaterstaat and SBRCURnet (CUR). Within this initiative physical model tests were initiated by Deltares, Boskalis and Van Oord. These model tests were focussed on a layer of rock on top of a 1:7 sandy bed. The physical model tests and the analysis of these tests are the topic of the present paper.

## EXPERIMENTAL SET-UP

The objective of the physical model tests was to gather data on the physical processes within a granular filter that trigger the erosion process, on (critical) hydraulic gradients at the sloping interface of sand and filter, and on the amount of base material erosion and filter settlement. The tests were carried out in the Scheldt Flume of Deltares (110m long, 1.2m high and 1m wide). A 1:7 slope was used since this was considered to be a realistic slope for sand in practical applications with a submerged sandy slope. The sand slope was continued above the waterline to ensure an even erosion process. Furthermore, the applied constant filter layer thickness over the slope allowed for a systematic investigation of the involved hydraulic gradients and erosion processes. The tests were performed with a fixed filter-base ratio of $D_{50,f}$ / $D_{50,b}$ = 250 (where $D_{50,f}$ is the filter material diameter of which 50%, by mass, is smaller and $D_{50,b}$ is the corresponding base material diameter) and single-layer filters of varying thickness. The chosen filter thicknesses were $d_f$ = 2.2, 4.4, 6.7 and 8.9 $D_{50,f}$. A wide filter grading was used to simulate field conditions. The sand material was kept the same in all tests.

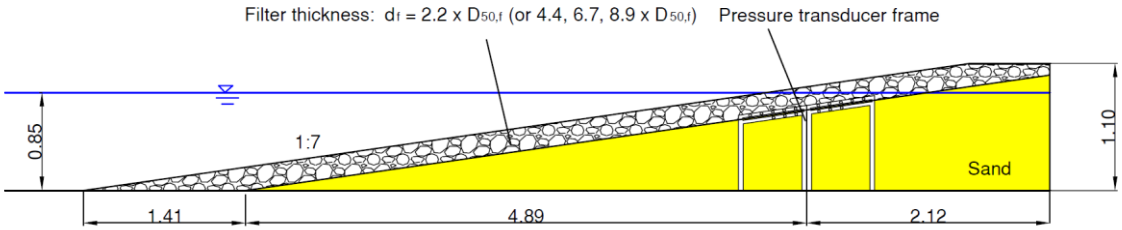


**Figure 1. Model set-up for basic tests in the Scheldt Flume of Deltares.**

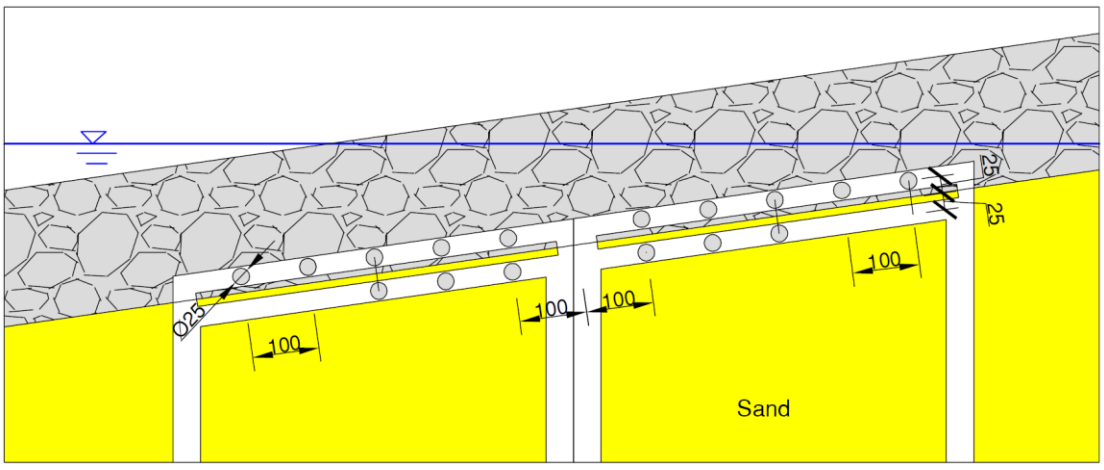


**Figure 2. Set-up of pressure sensors at the filter-sand interface (dimensions in mm).**

The following materials have been used in the tests:

- $D_{50,b}$ = 0.18 mm (base material)
- $D_{50,f}$ = 45 mm ($D_{n50,f}$ = 38 mm), $D_{15,f}$ = 20 mm, $D_{85,f}$ = 129 mm (filter material)
- $D_{50,f}$ / $D_{50,b}$ = 250
- $d_f$ / $D_{50,f}$ = 2.2, 4.4, 6.7, 8.9
- $D_{85,f}$/ $D_{15,f}$ = 6.5 (very wide grading)
- $n_f$ = 0.35
- $\rho_f$ = 2691 kg/m$^3$, $\rho_s$ = 2650 kg/m$^3$ (density of filter and sand material)

The porosity $n_f$ of the filter was determined in two ways: by calculation using the filter grading parameters and by measurement. Based on these methods a value of $n_f = 0.35$ was found for the filter porosity.

The test programme consisted of 24 tests of 3 hours duration (model) with various filter thicknesses ($d_f$ = 2.2, 4.4, 6.7 and 8.9 $D_{50,f}$). In addition a long duration test ($d_f$ = 4.4 $D_{50,f}$, 9 hours duration) was performed and two tests with a geotextile layer between sand and filter (3 hours duration); the latter are not reported here. The long duration test was performed to investigate the occurrence of a possible equilibrium situation in the erosion process.

Measurements were performed of the incident waves, the base material (sand) erosion and filter (surface) settlement using a mechanical profiler (6 individual profiles were measured over the flume width of 1m; the distance between the individual profiles was 0.143 m) and of the pressures and hydraulic gradients at the sand-filter interface. The placed sensors allowed for the determination of both slope-parallel and perpendicular pressure gradients at the interface, see Figure 2. In this paper only the (more relevant) slope-parallel gradients in the filter are discussed.

A frame of 16 pressure transducers (10 sensors in the filter and 6 sensors in the sand below the filter-sand interface) was used. The transducers were placed 25mm above and 25 mm below the initial filter-sand interface and around the waterline where the strongest erosive forces were expected. After the first test the water level was increased from $h$ = 0.7 m to $h$ = 0.85 m (see section on test programme). The latter water level was kept for all subsequent tests ($h$ = 0.85 m). All sensors were now located just beneath the SWL and at the place of maximum net erosion, see Figure 2. The hydraulic gradients along the slope have been determined from the pressure signal in the following manner:

$$i(t) = \frac{p_{i+1}(t) - p_i(t)}{\Delta x} \qquad (1)$$

where $p_{i+1}$ [m] and $p_i$ [m] are adjacent pressure transducers and $\Delta x$ is the distance (along the slope) between the pressure transducers (all pressure sensors were set to zero at the start of each test with reference to SWL).

The entire outer profile (filter surface) was measured at the beginning and end of each test series of 4 tests (see Table 1). Between subsequent tests only a limited profile measurement was performed at the position where the maximum erosion was found. The profile of the interface (sand profile) was also measured at the beginning and at the end of each test series of 4 tests. To measure the sand profile, the filter material was carefully removed up to the sand surface. After the sand profile had been measured, the sand and filter layer were repaired.

Videos and photo recordings were made of all tests. Through the glass wall of the flume sand profile changes were monitored.

Waves up to a significant wave height of $H_{m0}$ = 0.2 m were generated. The spectral significant wave height $H_{m0}$ and the spectral wave period $T_{m-1,0}$ ($T_{m-1,0} = m_{-1}/m_0$) were obtained from the measured wave energy spectra. In Van Gent (2001) the wave period $T_{m-1,0}$ was found to appropriately describe the influence of wave energy spectra on wave run-up, while in later studies this wave period was found to be the most appropriate wave period for other coastal processes (wave overtopping, wave reflection, dune erosion, and the stability of rock slopes). In all tests a Jonswap wave spectrum has been applied. Each configuration was tested with a constant wave steepness, either $s_p$ = 0.015 or $s_p$ = 0.04 with $s_p = 2\pi H_{m0}/gT_p^2$. This corresponds to $s_{m-1,0}$ = 0.018 or $s_{m-1,0}$ = 0.048 respectively, with $s_{m-1,0} = 2\pi H_{m0} / gT_{m-1,0}^2$. The test duration was 3 or 9 hours (model). The water depth ($h$ = 0.85 m) was kept constant during all tests (except for Test T01).

The test programme is given in Table 1:

**Table 1. Test programme (basic tests: Series 1-3, long duration test: Series 4)**

| Series | Test | Test set-up | | | Wave conditions | | | | | | | |
|---|---|---|---|---|---|---|---|---|---|---|---|---|
| | | $d_f$ (m) | $d_f/D_{50,f}$ (-) | $h$ (m) | $H_{m0}$ (m) | $T_p$ (m) | $T_{m-1,0}$ (s) | $s_p$ (-) | $s_{m-1,0}$ (-) | $\xi_p$ (-) | $\xi_{m-1,0}$ (-) | $t_{Tot}$ (hrs) |
| 1A | T01 | 0.2 | 4.4 | 0.70 | 0.08 | 1.9 | 1.7 | 0.014 | 0.017 | 1.2 | 1.1 | 3 |
| | T02 | 0.2 | 4.4 | 0.85 | 0.12 | 2.3 | 2.1 | 0.015 | 0.018 | 1.2 | 1.1 | 3 |
| | T03 | 0.2 | 4.4 | 0.85 | 0.16 | 2.6 | 2.4 | 0.015 | 0.018 | 1.2 | 1.1 | 3 |
| | T03ex | 0.2 | 4.4 | 0.85 | 0.20 | 2.9 | 2.6 | 0.015 | 0.018 | 1.2 | 1.1 | 3 |
| 1B | T04 | 0.2 | 4.4 | 0.85 | 0.08 | 1.1 | 1.1 | 0.039 | 0.043 | 0.7 | 0.7 | 3 |
| | T05 | 0.2 | 4.4 | 0.85 | 0.12 | 1.4 | 1.3 | 0.041 | 0.045 | 0.7 | 0.7 | 3 |
| | T06 | 0.2 | 4.4 | 0.85 | 0.16 | 1.6 | 1.5 | 0.040 | 0.044 | 0.7 | 0.7 | 3 |
| | T06ex | 0.2 | 4.4 | 0.85 | 0.20 | 1.8 | 1.7 | 0.040 | 0.045 | 0.7 | 0.7 | 3 |
| 2A | T07 | 0.4 | 8.9 | 0.85 | 0.08 | 1.8 | 1.7 | 0.015 | 0.018 | 1.2 | 1.1 | 3 |
| | T08 | 0.4 | 8.9 | 0.85 | 0.12 | 2.3 | 2.1 | 0.015 | 0.018 | 1.2 | 1.1 | 3 |
| | T09 | 0.4 | 8.9 | 0.85 | 0.16 | 2.6 | 2.4 | 0.015 | 0.018 | 1.2 | 1.1 | 3 |
| | T09ex | 0.4 | 8.9 | 0.85 | 0.20 | 2.9 | 2.6 | 0.015 | 0.018 | 1.2 | 1.1 | 3 |
| 2B | T10 | 0.4 | 8.9 | 0.85 | 0.08 | 1.1 | 1.1 | 0.038 | 0.042 | 0.7 | 0.7 | 3 |
| | T11 | 0.4 | 8.9 | 0.85 | 0.12 | 1.4 | 1.3 | 0.041 | 0.045 | 0.7 | 0.7 | 3 |
| | T12 | 0.4 | 8.9 | 0.85 | 0.16 | 1.6 | 1.5 | 0.040 | 0.045 | 0.7 | 0.7 | 3 |
| | T12ex | 0.4 | 8.9 | 0.85 | 0.20 | 1.8 | 1.7 | 0.041 | 0.045 | 0.7 | 0.7 | 3 |
| 3A | T13 | 0.3 | 6.7 | 0.85 | 0.08 | 1.8 | 1.7 | 0.015 | 0.018 | 1.2 | 1.1 | 3 |
| | T14 | 0.3 | 6.7 | 0.85 | 0.12 | 2.2 | 2.1 | 0.015 | 0.018 | 1.2 | 1.1 | 3 |
| | T15 | 0.3 | 6.7 | 0.85 | 0.16 | 2.6 | 2.4 | 0.015 | 0.018 | 1.2 | 1.1 | 3 |
| | T15ex | 0.3 | 6.7 | 0.85 | 0.20 | 2.9 | 2.6 | 0.015 | 0.018 | 1.2 | 1.1 | 3 |
| 3B | T16 | 0.1 | 2.2 | 0.85 | 0.08 | 1.8 | 1.7 | 0.015 | 0.018 | 1.2 | 1.1 | 3 |
| | T17 | 0.1 | 2.2 | 0.85 | 0.12 | 2.3 | 2.1 | 0.015 | 0.018 | 1.2 | 1.1 | 3 |
| | T18 | 0.1 | 2.2 | 0.85 | 0.16 | 2.6 | 2.4 | 0.015 | 0.018 | 1.2 | 1.1 | 3 |
| | T18ex | 0.1 | 2.2 | 0.85 | 0.20 | 2.9 | 2.6 | 0.015 | 0.018 | 1.2 | 1.1 | 3 |
| 4 | T19 | 0.2 | 4.4 | 0.85 | 0.20 | 2.9 | 2.6 | 0.016 | 0.019 | 1.1 | 1.0 | 9 |

where:

$H_{m0}$ : significant wave height (m)
$T_p$ : wave period at peak of spectrum (s)
$T_{m-1,0}$ : spectral wave period, $T_{m-1,0} = m_{-1}/m_0$ (s)
$s_p$, $s_{m-1,0}$ : wave steepness based on $T_p$ and $T_{m-1,0}$ respectively (-)
$\xi_p$, $\xi_{m-1,0}$ : Iribarren number / surf-similarity number based on $T_p$ and $T_{m-1,0}$ respectively (-)
$t_{Tot}$ : duration of test (hrs).

## OBSERVATIONS

The tests showed considerable sand accretion within the filter and erosion of the sand core (see *e.g.* Figure 3). The accretion within the filter reached a length of up to 1.8 m with a height of 100 mm (= 2.2 $D_{50,f}$) while the maximum observed erosion of the sand layer was approximately 1 $D_{50,f}$ (for the investigated case of $d_f$ = 4.4 $D_{50,f}$). The erosion took place at/just beneath the SWL ($h$ = 0.85 m). Initiation of sand motion along the interface of sand and filter was observed in all tests. Sand movement was generally observed along most of the structure slope, starting at the wave breaking point and reaching down to the flume bottom. The transport of sand was mostly in the form of sand clouds in the filter (only limited transport along the sand-filter interface), although some sand clouds were also seen to be transported through the filter layer into the water column (resulting in a water column saturated with fine sand). It was also observed that the transport of sand for thicker filter layers ($d_f$ = 4.4 – 8.9 $D_{50,f}$) is apparently not strongly related to wave impact phenomena; the wave rundown in the filter (which occurs significantly later than the wave impact) determines the sand transport down the slope, and seems to be mainly dependent on the volume of transported water (wave volume), not the type of wave breaking.

The long duration test (9 hours), conducted for $d_f$ = 4.4 $D_{50,f}$ (with $s_{op}$ = 0.015), showed that the erosion (sand transport) slowed down over time although an equilibrium condition was not reached during testing.

The sand erosion and accretion zone was found to coincide with the breaker zone (upper limit: point where the SWL crosses the sand interface; lower limit: 2 to 3 $H_{s,max}$ below SWL, whereby 1.25 - 2 $H_{s,max}$ below SWL is the lower limit for the erosion zone and 3 $H_{s,max}$ below SWL is the lower limit for the accretion zone as found in the tests).

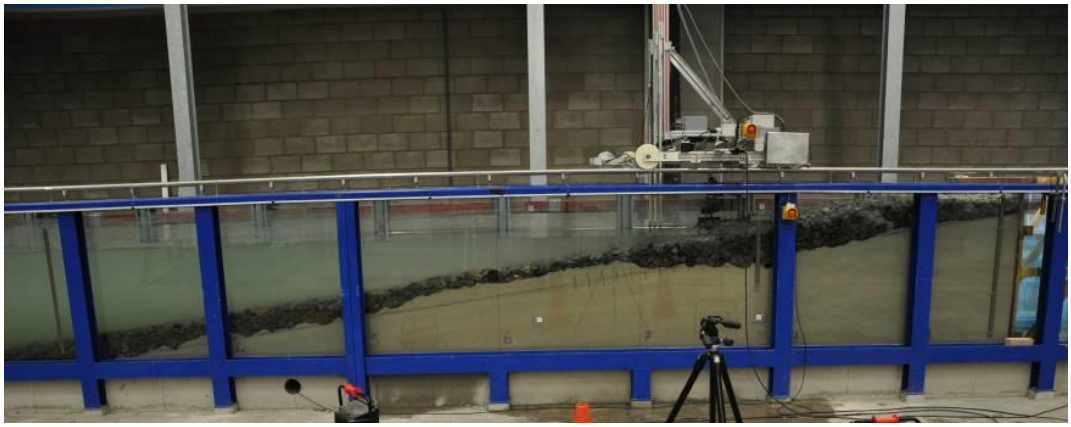

**Figure 3a. Typical sand erosion profile (after Test T03ex).**

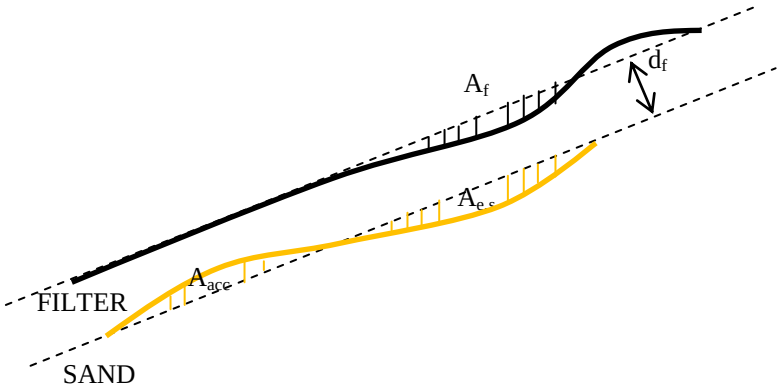


**Figure 3b. Typical erosion and accretion pattern (parameter definition).**

### Special filter test case $d_f$ = 2.2 $D_{50,f}$

The erosion trends found for a filter thickness of $d_f$ = 2.2 $D_{50,f}$ differed strongly from all other investigated filter thicknesses due to changing physical processes in the filter layer. Large amounts of sand were directly entrained (sucked out) into the water column through the filter layer (failure of filter function). The entrained sand settled later on top of the stones along the entire (2D) slope. The latter is due to a model effect: in reality the entrained sand in the water column is transported along the shore and does not necessarily settle in the same cross-section. The measured filter/sand profiles for $d_f$ = 2.2 $D_{50,f}$ can therefore not be compared with the previous test series where no strong sand entrainment into the water column took place (although sand transport through the filter did occur). It should be mentioned that the stone cover remained intact during the tests (no exposure of sand layer due to stone removal). Physically, the wave impact force had a much stronger influence on the sand entrainment in the tests with $d_f$ = 2.2 $D_{50,f}$. The wave tongue was observed to directly penetrate the filter layer up to the sand surface, causing a seaward current and large vortices at the impact location. Furthermore, the influence of the wave suction forces on the sand bottom were clearly visible (*e.g.* below the incoming wave trough and just before the plunging wave hits the structure). Since the strong suction forces caused large amounts of sand to be directly transported through the filter into the water column, transport of sand material through the filter played a less significant role. The observed sand accretion within the filter did not increase significantly (approximately 1 $D_{50,f}$, *i.e.* half the filter thickness) after completion of the tests, since the sand was mostly entrained directly into the water column and settled later over a wide region. This resulted in a large increase in accretion length, but not in accretion height.

### Filter settlement and sand erosion

When the size of the filter settlement area $A_f$ is compared with the sand erosion area $A_{e,s}$, see Table 2 and Figure 3b, it is apparent that the magnitude can differ substantially. Please note that the area of filter settlement $A_f$ has here been corrected for the occurred damage (rock displacement due to waves).

**Table 2. Comparison of area of filter settlement ($A_f$) and measured area of sand erosion ($A_{e,s}$) and area of sand accretion ($A_{acc}$)**

| TEST | $A_f$ [m$^2$] | $A_{e,s}$ [m$^2$] | $A_{acc}$ [m$^2$] | $A_f / A_{e,s}$ [-] | $n_f = A_{e,s} / A_{acc}$ [-] |
|---|---|---|---|---|---|
| T03ex | 0.056 | 0.033 | 0.167 | 1.698 | 0.199 |
| T06ex | 0.040 | 0.018 | 0.121 | 2.238 | 0.148 |
| T09ex | 0.013 | 0.016 | 0.056 | 0.839 | 0.275 |
| T12ex | 0.013 | 0.022 | 0.024 | 0.592 | 0.903 |
| T15ex | 0.024 | 0.029 | 0.117 | 0.830 | 0.252 |
| T18ex | 0.046 | 0.023 | 0.099 | 2.025 | 0.229 |
| T19 | 0.087 | 0.096 | 0.233 | 0.900 | 0.414 |
| T20b | 0.021 | 0.006 | 0.017 | 3.665 | 0.333 |

Generally, it is therefore advisable to differentiate between areas of filter (stone) settlement and areas of sand erosion, since the settlement of the filter layer can only provide a first estimate of the damage to the sand layer beneath. The observations also showed that the maximum sand erosion and filter settlement did not always occur at the same spot. However, since the tests provided more data on filter settlement (a measurement was performed after each test in contrast to the sand erosion measurement which was only performed after each series of four tests) and less direct sand erosion measurements, the filter settlement data were also included in the analysis (as an indication of the erosion trend, see Equation 2; the absolute settlement values were not used). Despite the uncertainty (in the absolute values of $A_f / A_{e,s}$), the filter data showed in many cases similar trends as the sand data (see Figure 5a).

Another important aspect to address is the relationship between the sand accretion area $A_{acc}$ in the filter and the sand erosion area $A_{e,s}$, see Table 2 and *e.g.* Figure 3 (which shows the accretion and erosion zones within the filter after testing). From Table 2 it is apparent that the sand erosion volumes (areas) did not correspond to the sand accretion values within the filter. The measured sand erosion volumes were significantly smaller. The main reason for this observation is that sand accretion occurs in the pores of the filter stone layer, while the sand erosion occurs over the entire sand bed. The sand accretion volume could therefore be expected to be approximately $1/n_f \approx 3$ times larger than the sand erosion volume. However, the factor between sand accretion and sand erosion volumes was not constant for all tests and higher than expected ($1/n_f$ = 3.6 to 6.7 for most tests, instead of 3), see the last column of Table 2. For Test T12ex the size of the accretion area was close to that of the erosion area. Please note that the expected $n_f$ values (last column of Table 2) are somewhat smaller than the measured values respectively those derived from the filter grading curve ($n_f$ = 0.35). Aspects that might have caused this variation in $n_f$ (and erosion volumes) are:

- Local changes in filter porosity (also over time).
- Since many stones settled within the sand, the sand surface increased somewhat in height (by way of volume conservation) during testing, which counteracted the erosion. This way the measured sand erosion is somewhat underestimated. However, how much is unclear, since the amount (volume) of stones within the sand was not measured.
- Please note that similar observations (a net 'increase' in sediment/sand volume during testing) have already previously been made in dune erosion tests, see *e.g.* Coeveld (2004). In this case the measured net 'increase' in sand volume was attributed to changes in sand porosity (bulk density) during the tests (*e.g.* deposited sand was more loosely packed).

## TEST RESULTS

In the subsequent graphs (Figures 4 and 5) each data point (for the sand erosion data) corresponds to a test series of 4 tests (total test series duration is 12 hours). This is due to the fact that sand erosion measurements (profiles) were only performed at the end of each test series, after the filter layer had been removed. Note that the sand erosion/accretion is made dimensionless using $d_f$ instead of $D_{n50,f}$ (*i.e.* $A_{e,s} / d_f^{\,2}$ instead of $S = A_{e,s} / D_{n50,f}^{\,2}$). For the erosion of the sand layer this seems more appropriate than using the median filter stone diameter, since the sand erosion (accretion) proved to be primarily dependent on $d_f$.

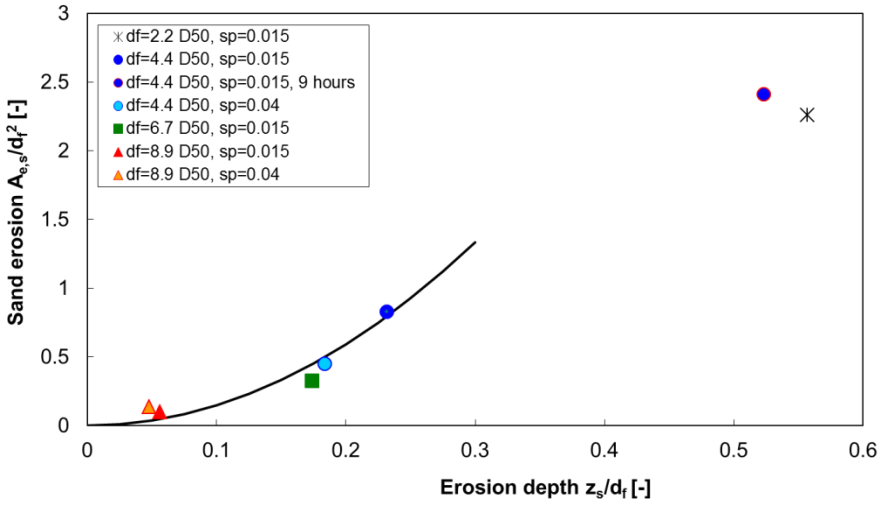


**a. Sand erosion area versus erosion depth $z_s/d_f$**

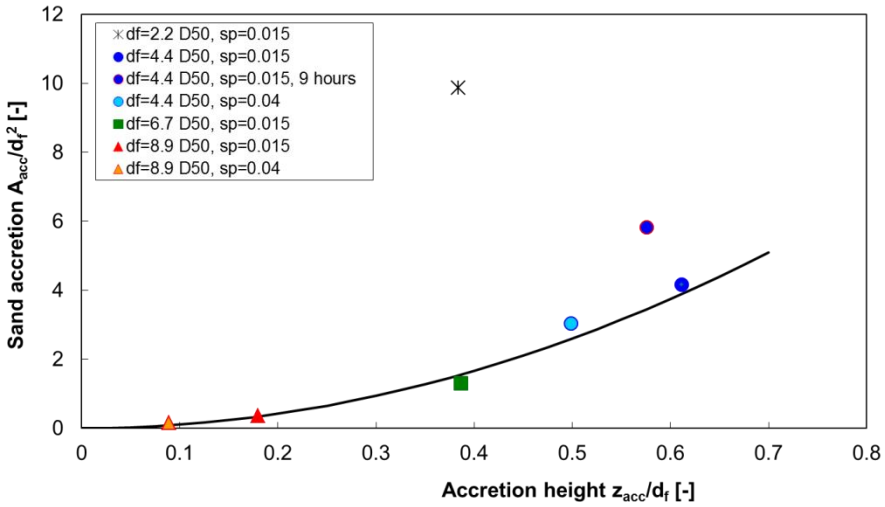


**b. Sand accretion area versus accretion height $z_s/d_f$**

**Figure 4. Sand erosion depth and sand accretion height**

In Figure 4a the relative sand erosion area is plotted against the relative erosion depth $z_s/d_f$ ($z_s$ = erosion depth measured perpendicular to sand-filter interface). It can be seen that the maximum erosion depth (sand) increases with the area of sand erosion. The same is valid for the accretion height $z_{acc}$ ($z_{acc}$ measured perpendicular to sand-filter interface) and the accretion area, see Figure 4b. Please note that no clear dependency of sand erosion/accretion on wave steepness has been found.

From Figure 4 it is apparent that the sand erosion volumes do not correspond to the sand accretion volumes. The accretion volume is 3.6 to 6.7 times larger than the erosion volume. The most significant reason for this fact is that sand accretion occurs in the pores of the filter stone layer, while the sand erosion occurs over the entire sand bed. The data for the thinnest filter layer, $d_f$ = 2.2 $D_{50,f}$, and for the long duration test (9 hours, while all other individual tests have a duration of 3 hours) are presented in Figure 4 as well. This has been done for the sake of completeness. However, the trends found for the thin filter layer ($d_f$ = 2.2 $D_{50,f}$) differ strongly from all other tested filter thicknesses. This is due to the occurrence of different dominant processes during the test. The trends for the thin filter layer ($d_f$ = 2.2 $D_{50,f}$) are therefore not considered to be representative and are not included in the derived formulae. The long duration test (which was performed to investigate a possible equilibrium situation) is also not included, since it cannot be directly compared with the other tests.

The relationship between the sand erosion area $A_{e,s}/d_f^{\,2}$ and the hydraulic gradient $i_{I,N,2\%}/i_{cr}$, as shown in Figure 5, is based on the most reliable pressure sensor results (transducers in the filter layer, top row). In this figure the 2% exceedance values of the hydraulic gradient parallel to the interface, $i_{I,N,2\%}$, is calculated over all tests within a test series (*e.g.* T01-T03 or T04-T06); all tests were combined to one file (denoted by subscript *N*) from which the 2% exceedance value was determined. This was done for each pair of transducers separately, and the average was then calculated over all transducer pairs. The critical hydraulic gradient $i_{cr}$ (for a sloped filter structure) can be calculated using Equations 7-9 ($i_{cr} \approx 0.042$).

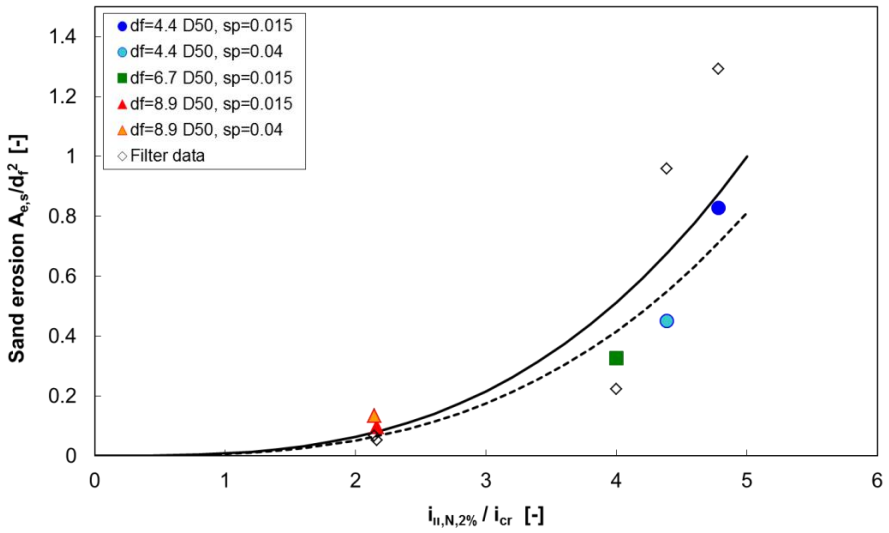


**a. Sand erosion**

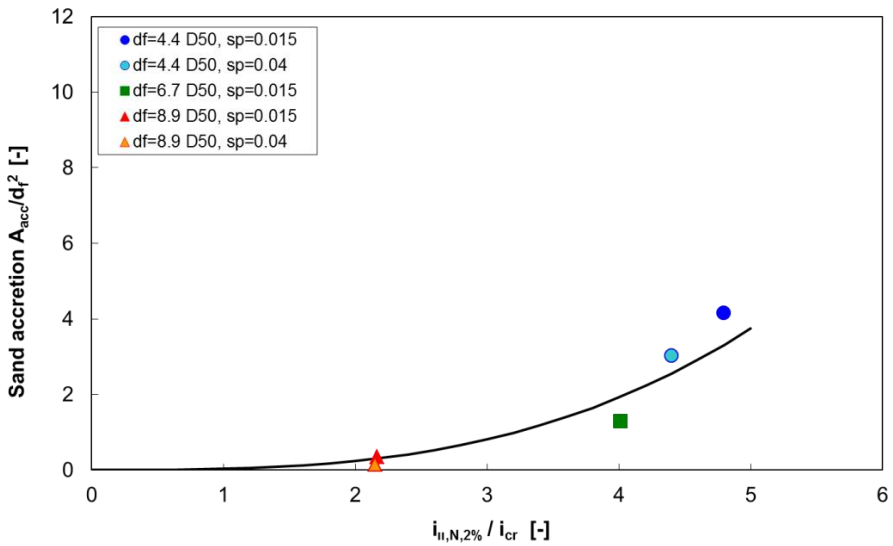


**b. Sand accretion**

**Figure 5. Sand erosion and sand accretion versus slope parallel gradients for $i_{cr}$ = 0,04 and $n_f$ = 0.35**

Figure 5 shows that the erosion increases with the measured hydraulic gradient. Similarly to the previous results, the effect of filter thickness is most pronounced. The dotted line in Figure 5 represents the trend based on the sand erosion data; the continuous line (Equation 2) gives the trend for the combined data set of sand erosion data and filter erosion data (see previous section on observations/filter settlement).

The filter data have been added in Figure 5a, since they generally support the *trend* found for the sand erosion data and provide additional information (note that for the accretion area and erosion depth, as presented in Figures 4a/b, this comparison was not possible). Equation 2 has been deliberately derived for a combination of sand erosion and filter data, resulting in a more conservative assessment of the erosion area (and erosion depth). In Figure 5, Test series 3b, with $d_f = 2.2\ D_{50,f}$, is not shown since the values lie far outside the borders ($i_{l,2\%}/i_{cr} = 20.3$, $A_{e,s}/d_f^{\,2}=2.3$). The same is valid for Figure 6 ($i_{l,2\%} = 0.31\text{-}0.86$, $H_{m0}/d_f = 0.8\text{-}2$).

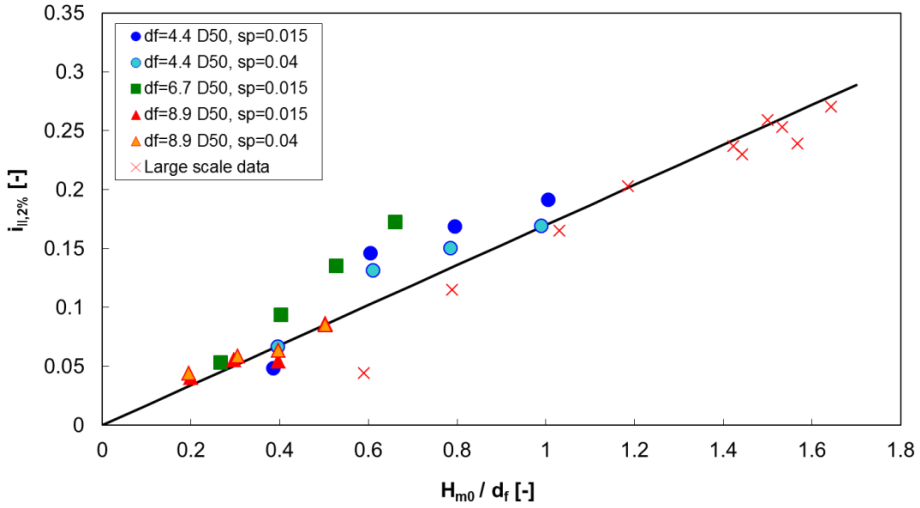


**a. Relative wave height as function of $d_f$, plotted against hydraulic gradient ($i_{l,2\%}$)**

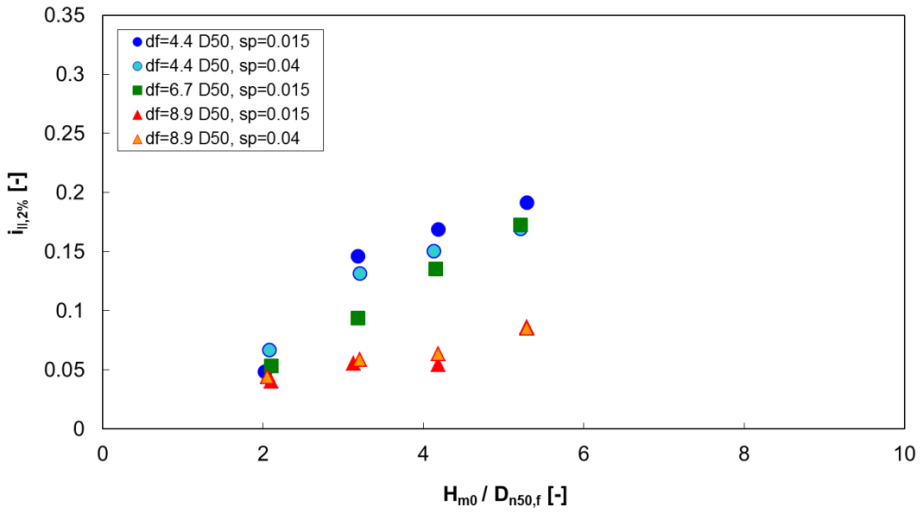


**b. Relative wave height as function of $D_{n50,f}$, plotted against hydraulic gradient ($i_{l,2\%}$)**

**Figure 6. Relative wave height plotted against hydraulic gradient ($i_{l,2\%}$)**

In Figure 6 the relative wave height is plotted against the hydraulic gradient parallel to the sand-filter interface ($i_{l,2\%}$). For this graph it was *not* necessary to use the $i_{l,N,2\%}$ values (*i.e.* determined over the entire test series), since the data were not compared with erosion data. Instead, the values per test could be used. Added are also results of large scale tests at Deltares on a filter structure on sand. That model investigation was performed with similar geometries and filter/sand properties: slope 1:7.5, wide gradation $D_{85,f}/D_{15,f}$ = 135 mm / 20 mm = 6.75, but with a significantly larger filter thickness $d_f/D_{50,f}$ ~ 50-58 ($H_{m0}/d_f$ = 0.6 - 1.6). The large scale tests were performed in the Delta Flume of Deltares. Some base material erosion appeared to have occurred during the tests, although the effect

seemed limited and was not measured in detail. The upper range of $i_{l,2\%}$ in Figure 6a, which represents strong base material erosion, can thus not exactly be determined, although the large scale tests indicate that it is located somewhere above $i_{l,2\%} >> 0.25$ ($i_{l,2\%}/i_{cr} >> 8$). The observed trend in Figure 6a (Equation 6) shows a very good correlation ($R^2 = 0.91$) over both small and large scale tests, indicating that the hydraulic gradient at the interface of filter stones and sand can be correctly estimated using the relative wave height ($H_{m0}/d_f$).

Please note that the hydraulic gradient appears to be much stronger correlated to the filter thickness $d_f$ than the filter material diameter $D_{n50,f}$, see Figure 6b. Furthermore, in Figure 6b the large scale data lie far outside the borders ($H_{m0}/D_{n50,f} = 39 - 108$). A similar trend for small and large scale data as in Figure 6a could thus not be established for $H_{m0}/D_{n50,f}$.

## EROSION PREDICTION

The following parameters have been identified to describe the sand erosion and sand accretion at the sand-filter interface:

- Erosion and accretion area: $A_{e,s}/d_f^2$ and $A_{acc}/d_f^2$:
- Erosion depth and accretion height: $z_s/d_f$ and $z_{acc}/d_f$:
- Loading parameter: $i_{\parallel,2\%}/i_{cr}$

where

$A_{e,s}$ : eroded area of sand (base material) ($m^2$)
$A_{acc}$ : area of sand accretion ($m^2$)
$d_f$ : filter thickness (m)
$z_{acc}$ : sand accretion measured perpendicular to sand-filter interface (m)
$z_s$ : settlement measured perpendicular to sand-filter interface (m)
$i_{\parallel,2\%}$ : hydraulic gradient, parallel to the sand-filter interface, exceeded by 2% of waves (-)
$i_{cr}$ : critical hydraulic gradient (-)

The best parameter to describe the hydraulic loading at the filter-sand interface (which determines the transport of base material and the erosion process) appears to be the hydraulic gradient along the filter-sand interface, here described as the slope parallel gradient that is exceeded by 2% of the incident waves ($i_{l,2\%}$). This hydraulic gradient was found to be directly proportional to the incident wave loading and the thickness of the filter layer ($H_{m0}/d_f$). By dividing this gradient by the critical hydraulic gradient, which describes the onset of base material motion (as described *e.g.* by De Graauw, 1983), the hydraulic loading becomes a function of $n_f$ (porosity of filter material), $D_{15,f}$ (filter material), $D_{50,b}$ (sand), the wave load ($H_{m0}$) and the thickness of the filter ($d_f$). It is noted that the described loading parameter also appear to be applicable to current loading (see *e.g.* Wolters & Van Gent, 2012).

Base material erosion and accretion of sand within the filter layer can be described in two ways: in form of an erosion depth (and accretion height) or in form of an erosion area (and accretion area). The erosion area (typically used in many design guidelines on rock, see *e.g.* the Rock Manual) is a frequently used parameter. Please note that the data from the physical model tests indicate that a relatively reliable relationship between $A_{e,s}/d_f^2$ and $z_s/d_f$ (or $A_{acc}/d_f^2$ and $z_{acc}/d_f$) exists, so that the erosion depth (accretion height) can be directly determined from the erosion area (accretion area).

Both erosion depth and erosion area (as well as accretion height and accretion area of sand within the filter layer) are described as a function of the filter thickness $d_f$. This parameter was determined in the physical model tests to be the most relevant filter parameter. Erosion and accretion both show a much weaker dependency on *e.g.* the filter stone diameter ($D_{50,f}$ or $D_{15,f}$).

Based on the model tests, the following relationships were developed for base material (sand) erosion and accretion of sand in open granular filters under perpendicular wave attack on a 1:7 slope:

Sand erosion:

$$\frac{A_{e,s}}{d_f^2} = 0.008\left(\frac{i_{||,2\%}}{i_{cr}}\right)^3 \tag{2}$$

Accretion:

$$\frac{A_{acc}}{d_f^2} = 0.03\left(\frac{i_{||,2\%}}{i_{cr}}\right)^3 \tag{3}$$

Erosion depth (with $A_{e,s}/d_f^2$ from Equation 2):

$$\frac{z_s}{d_f} = 0.26\left(\frac{A_{e,s}}{d_f^2}\right)^{0.5} \tag{4}$$

Accretion height (with $A_{acc}/d_f^2$ from Equation 3):

$$\frac{z_{acc}}{d_f} = 0.31\left(\frac{A_{acc}}{d_f^2}\right)^{0.5} \tag{5}$$

with

$$i_{||,2\%} = 0.17\frac{H_{m0}}{d_f} \tag{6}$$

where

$A_{e,s}$ : eroded area of sand (base material) ($m^2$)
$A_{acc}$ : area of sand accretion ($m^2$)
$d_f$ : filter thickness (m)
$H_{m0}$ : significant wave height (m)
$i_{||,2\%}$ : hydraulic gradient, parallel to the sand-filter interface, exceeded by 2% of waves (-)
$i_{cr}$ : critical hydraulic gradient (-)
$z_{acc}$ : sand accretion measured perpendicular to sand-filter interface (m)
$z_s$ : settlement measured perpendicular to sand-filter interface (m)

The value for $i_{cr}$ describing the initiation of motion under steady flow parallel to the interface between sand and filter can be determined with Equations 7-9 (CUR 161, 1993; Klein Breteler *et al.*, 1992) for 0.1mm < $D_{50,b}$ < 1mm and sloped filter structures. The approach is based on the Forchheimer equation and the critical filter velocity $u_{f,cr}$. Although originally not developed for cyclic flow (waves), the equations are also assumed to be valid for wave loading conditions (see Klein Breteler *et al.* 1992). This assumption has been confirmed in the present study, which showed initiation of motion for $i/i_{cr} \approx 1$. Similar observations were already made in Wolters & Van Gent (2012). For more information on the Forchheimer relation as applied to granular filters, reference is made to Wolters (2012) and Van Gent (1995).

$$i_{cr} = a_f \cdot u_{f,cr} + b_f \cdot u_{f,cr}^2 \tag{7}$$

$$u_{f,cr} = \left[\frac{n_f}{c}\left(\frac{D_{15,f}}{v_w}\right)^m \sqrt{\psi g \Delta_b D_{50,b}\left(\frac{\sin(\phi-\alpha)}{\sin(\phi)}\right)}\right]^{\frac{1}{(1-m)}} \tag{8}$$

where Klein Breteler *et al.* (1992) used:

$$a_f = \frac{160\cdot\nu\cdot\left(1-n_f\right)^2}{g\cdot n_f^3\cdot D_{f,15}^2} \quad \text{and} \quad b_f = \frac{2.2}{g\cdot n_f^2\cdot D_{f,15}} \tag{9}$$

where:

$i_{cr}$ : critical hydraulic gradient (-)
$n_f$ : porosity of filter material (-)
$D_{15,f}$ : filter material diameter (m) of which 15% (by mass) is smaller (m)
$D_{50,b}$ : base material diameter (m) of which 50% (by mass) is smaller (m)
$\phi$ : angle of repose of base material (˚)
$\alpha$ : bed slope (˚)
$a_f$ : linear friction coefficient of the filter (s/m)
$b_f$ : quadratic friction coefficient of the filter ($s^2/m^2$)
g : gravitational acceleration ($m^2/s$)
$\nu_w$ : kinematic viscosity of water ($m^2/s$)
$c,m,\psi$ : coefficients (see Table 3)
$\Delta_b$ : relative density of the base material (-)

**Table 3. Parameters in the formula for the critical filter velocity**

| $D_{b50}$ (mm) | c (-) | m (-) | $\psi$ (-) |
|---|---|---|---|
| 0.1 | 1.18 | 0.25 | 0.11 |
| 0.15 | 0.78 | 0.2 | 0.073 |
| 0.2 | 0.71 | 0.18 | 0.055 |
| 0.3 | 0.56 | 0.15 | 0.044 |
| 0.4 | 0.45 | 0.11 | 0.038 |
| 0.5 | 0.35 | 0.07 | 0.036 |
| 0.6 | 0.29 | 0.04 | 0.034 |
| 0.7 | 0.22 | 0 | 0.034 |
| 0.8 | 0.22 | 0 | 0.034 |
| 1.0 | 0.22 | 0 | 0.035 |

By taken into account Equations 2, 3 and 6, Equations 4 and 5 can be re-written as follows:

Erosion depth:

$$z_s = 0.0016\left(\frac{H_{m0}^{1.5}}{d_f^{0.5}\cdot i_{cr}^{1.5}}\right) \tag{10}$$

Accretion height:

$$z_{acc} = 0.0038\left(\frac{H_{m0}^{1.5}}{d_f^{0.5}\cdot i_{cr}^{1.5}}\right) \tag{11}$$

Based on a chosen wave height $H_{m0}$ and filter thickness $d_f$ the accretion height $z_{acc}$ (and erosion depth $z_s$) can be directly determined with Equations 10 and 11. The critical hydraulic gradient $i_{cr}$ should again be determined via Equations 7-9.

The correlation of the derived formulae with the underlying data has been assessed by determining the confidence bounds for the correlation coefficient using the Fisher transformation and a significance value of $\alpha$ = 5%. For Equations 2 to 6 the correlation coefficient varies between $R$ = 0.93 and $R$ = 0.99. The lower bound of the confidence interval varies between $R_l$ = 0.63 and $R_l$ = 0.90. The accuracy of the formulae is therefore considered acceptable given the limited data available.

The presented equations are valid for the following boundary conditions (validity ranges):

- $z_{acc} / d_f < 0.6$ ($A_{acc} / d_f^2 < 4$)
- $z_s / d_f < 0.25$ ($A_{e,s} / d_f^2 < 1$)
- $0.32 < n_f < 0.38$
- $H_{m0} / \Delta D_{50,f} < 4$
- $4 < d_f / D_{50,f} < 9$
- 1:7 slope
- $D_{85,f} / D_{15,f} = 6.5$
- $d_f / H_{m0} = 1 - 5.1$
- $i_{l,2\%} / i_{cr} < 8.3$
- Storm durations of up to 14000 waves.

Application of the proposed equations outside these ranges is not recommended, since supporting data is currently not available. For the range of the filter porosity ($0.32 < n_f < 0.38$) a narrow bandwidth (+/- 10%) around the tested value ($n_f = 0.35$) is considered acceptable. The tested range of the stability parameter was: $H_{m0} / \Delta D_{50,f} < 4$ (stable rock slopes). The validity outside this range cannot be guaranteed, in any case not for $H_{m0} / \Delta D_{50,f} > 6$ (dynamic rock slopes). The tested range of the filter thickness was $4 < d_f / D_{50,f} < 9$. The tests showed that for filter thicknesses equal or smaller than 2 the found relationships are not valid (the hydraulic processes in the filter layer change). There is no indication that the erosion trends might change for filter thicknesses above $d_f / D_{50,f} > 9$. The investigated conditions were limited to a 1:7 structure slope and a wide filter gradation ($D_{85,f} / D_{15,f} = 6.5$). Application to other structure slopes and material gradations is not recommended. So far not included is a potential dependency on parameters such as varying material density, material gradation, slope angle and filter composition (multiple filter layers). Furthermore, the influence of the breaker parameter (only plunging conditions were investigated) on the predicted erosion was limited. Therefore, the analysis of the potential influence of $\xi$ on sand erosion at the filter-sand interface was omitted in the study.

## USAGE OF FORMULAE

It is suggested to follow the following steps when using Equations 2 to 9 to predict the amount of erosion and accretion of sand at the filter-sand interface:

1. Based on a chosen wave height $H_{m0}$ and filter thickness $d_f$ the hydraulic gradient $i_{l,2\%}$ can be determined with Equation 6.
2. The critical hydraulic gradient $i_{cr}$ can be determined from Equations 7-9.
3. Based on the obtained $i_{2\%}$ and $i_{cr}$ (from Steps 1 and 2) the ratio $i_{l,2\%} / i_{cr}$ can be determined and from that the values for $A_{e,s} / d_f^2$ and $A_{acc} / d_f^2$ using Equations 2 and 3.
4. The corresponding values for $z_s / d_f$ and $z_{acc} / d_f$ can now be determined with Equations 4 and 5.
5. Finally, based on the chosen $d_f$ , the values for $z_s$ and $z_{acc}$ can be calculated (alternatively Equations 10 and 11 can be used). If the design criteria for $z_s$ and $z_{acc}$ are not met, the filter parameter(s) need to be adjusted and the equations applied anew (iterative procedure).

Based on the present study the amount of erosion and accretion can be determined. However, the present study does not provide guidelines on the amount of acceptable erosion and/or accretion (design criteria).

## CONCLUSIONS AND RECOMMENDATIONS

The application of open granular filters in rubble mound structures can reduce the number of filter layers compared to structures with geometrically tight filters. Since open filters have a large ratio of the size of the toplayer (*i.e.* a filter layer of rock) and the base material (*e.g.* sand), the minimum thickness of the filter layer needs to be determined in order to limit the erosion of base material and settlement of the filter layer. In order to improve the knowledge on the behaviour of open granular filters under wave loading, laboratory experiments have been conducted in the Scheldt Flume of Deltares. The physical model tests focussed on a sloped granular filter with a 1:7 slope where rock material was placed directly on sand. The rock material had a wide gradation ($D_{85,f} / D_{15,f} = 6.5$).

Based on the physical model tests formulae have been derived for the sand erosion and sand accretion at the filter-sand interface (*i.e.* rock-sand interface). The sand erosion and accretion depend on the wave height, the thickness of the filter layer and the critical hydraulic gradient at the filter-sand interface. The critical hydraulic gradient at the filter-sand interface depends on the size of the rock material, the size of the sand and the porosity of the rock layer.

Since the formulae are so far based on a limited number of experiments, it is recommended to perform additional validation at a large scale, and for 3D effects like oblique wave attack. The incorporation of data with other slope angles, other material gradings for both base and filter layer and with multiple filter layers is also recommended.

Based on the present study the amount of erosion and accretion at the filter-sand interface of open filters can be determined. However, the present study does not provide guidelines on the amount of acceptable erosion and/or accretion (design criteria). It is recommended to develop such design criteria for open filters.

**ACKNOWLEDGMENTS**

This research project has been performed in collaboration with various organisations. The authors wish to thank the following persons for their support and input: Coen Kuiper (Witteveen+Bos Consultants), Kees Dorst (Infram), Daan Heineke (RWS/GPO), Mark Franssen (RWS/GPO), Ger Vergeer (SBRCURnet), Teus Blokland (Gemeente Rotterdam), and Henk Verheij (Deltares).

**REFERENCES**

Bakker, K.J., Verheij, H.J., and De Groot, M.B., 1994, Design relationship for filters in bed protection, *J. Hydraulic Eng.*, 120(9), 1082-1088.

CIRIA, CUR and CETMEF, 2007, *The Rock Manual* (2nd edition), C683, CIRIA, London.

Coeveld, M.E., 2004, Model study on dune erosion, Report H4265, *Delft Hydraulics* (in Dutch).

CUR report 161, 1993, *Filters in hydraulic engineering*, Gouda (in Dutch).

CUR report 233, 2010, Interface stability of granular filter structures, Theoretical design methods for currents, *CURNET*, Gouda.

De Graauw, A., Van der Meulen, T., Van der Does de Bye M., 1983, Design criteria for granular filters, Publication 287, *Delft Hydraulics*.

Klein Breteler, M., Den Adel H., Koenders M.A., 1992, Placed (pitched) stone revetments, Filter design rules, report M1795/H195, XXI, *Delft Hydraulics & Geo Delft* (in dutch).

Van de Sande, S.A.H., 2012, Stability of open filter structures, MSc. Thesis, *Delft University of Technology*, Delft.

Van Gent, M.R.A., 1995, Porous flow though rubble mound material, *J. of Waterway, Port, Coastal and Ocean Engineering*, Vol.121, no.3, pp.176-181, ASCE, New York.

Van Gent, M.R.A., 2001. Wave run-up on dikes with shallow foreshores, *J. of Waterway, Port, Coastal and Ocean Engineering*, ASCE, Vol.127, No.5, Sept/Oct 2001, pp.254-262.

Wolters, G., 2012, Interface stability of granular filter structures, Design methods for open filters under wave loading (Desk study), project 1205012, *Deltares*.

Wolters, G. & Van Gent, M.R.A., 2012, Granular open filters on a horizontal bed under wave and current loading, *Proc. 33rd Conference on Coastal Engineering*, Santander, Spain, 2012.